

Machine learning phase transitions of the three-dimensional Ising universality class

Xiaobing Li,¹ Ranran Guo,¹ Kangning Liu,¹ Jia Zhao,¹ Fen Long,¹ Yu Zhou,² and Zhiming Li^{1,*}

¹*Key Laboratory of Quark and Lepton Physics (MOE) and Institute of Particle Physics,
Central China Normal University, Wuhan 430079, China*

²*University of California, Los Angeles, CA 90095, USA*

Exploration of the QCD phase diagram and the critical point is one of the main goals in current relativistic heavy-ion collisions. The QCD critical point is expected to belong to a three-dimensional (3D) Ising universality class. Machine learning techniques are powerful in distinguishing different phases of matter in an automated way and provide a new perspective on the study of phase diagram. We investigate phase transitions in the 3D cubic Ising model by using supervised learning methods. It is found that a 3D convolutional neural network can be trained to well predict physical quantities in different spin configurations. With a uniform neural network architecture, it can encode phases of matter and identify both the second- and the first-order phase transitions. The important features that discriminate different types of phase transitions in the classification processes are investigated. The method does not rely on order parameters or any other specific knowledge of thermodynamical variables of the system. Hence, it can be developed to study and understand the QCD phase transitions in relativistic heavy-ion collisions.

I. INTRODUCTION

One of the major goals in high energy heavy-ion collisions is to explore the QCD phase structure and the critical point [1–4]. Due to the fermion sign problem, Lattice QCD calculation is restricted to the region of vanishing or small baryon chemical potential (μ_B) and it predicts a crossover from hadronic phase to a Quark Gluon Plasma (QGP) phase in this area [5, 6]. The results of QCD based models indicate that the transition could be a first-order at large μ_B [7]. The point where the first-order phase transition ends is the critical point (CP) [8, 9]. This CP is proposed to be characterized by a second-order phase transition, which becomes a unique property of strongly interacting matter [10–13]. Attempts are being made to explore the CP and phase boundary both experimentally and theoretically [10–21].

The QCD equation of state with a CP is an essential ingredient for hydrodynamic simulations of fireball evolution in heavy-ion collision. Universality of critical phenomena allows us to predict the leading singularity of the QCD equation of state near CP [21]. Systems with different interactions, but with the same symmetry structure and having the same dimensionality, share the same critical behaviour. It is argued that the QCD CP belongs to the same Z(2) universality class [22, 23] as the three-dimensional (3D) Ising model [1, 24–27]. Therefore, universality makes the Ising model very relevant for studies of systems that display the Z(2) symmetry [28–31]. By means of a parametrization of the scaling equation of state in the 3D Ising model and a non-universal mapping, it allows to construct an equation of state matching the first principle Lattice QCD calculations and to include the proper scaling behavior in the proximity of the CP [11, 32–35]. It can also map the phase diagram

of the 3D Ising model onto the one of QCD [32, 36, 37]. Thus the CP, the lines of first-order phase transition and crossover in the 3D Ising model are related to those of QCD.

Classifying phases of matter and identifying phase transitions is one of the central topics in current phase structure investigations. In the conventional statistical method, it relies on the identification of order parameters or the analysis of singularities in the free energy and its derivatives. However, the order parameter of the QCD phase transition is hard to determine or difficult to measure in experiments. And some phases like topological ones [38, 39] do not have any clear order parameters because the symmetry that drives the phase transition is not manifest in the Hamiltonian. Therefore, it is important to develop new methods to identify phases in these systems. With the development of more powerful computers and artificial neural networks, machine learning (ML) [40, 41], a data-driven method, is proposed to be increasingly efficient for these studies. Deep neural networks, in particular, have been applied to recognize, classify, and characterize complex sets of data. Such methods have proved to be useful and strikingly successful for the investigation of complex physical problems [42, 43], like in the study of the QCD equation of states by classifying phase transition types [44–49], in the search for the order parameter of the nuclear liquid-gas phase transitions [50, 51], and in identifying phase transitions by circumventing the fermion sign problem [52]. One of the most promising advantages of deep learning is that it only requires raw low-level data, such as spin configurations, energy spectrum, or wave functions, so only elementary knowledge in physics is needed. With sufficiently large data sets, higher-level features can be recognized by various ML architectures [53] and then be used to identify phases.

In this work, we explore the ability of supervised learning method to discriminate phases and classify phase transitions according to configurations produced by a 3D

*Electronic address: lizm@mail.cnu.edu.cn

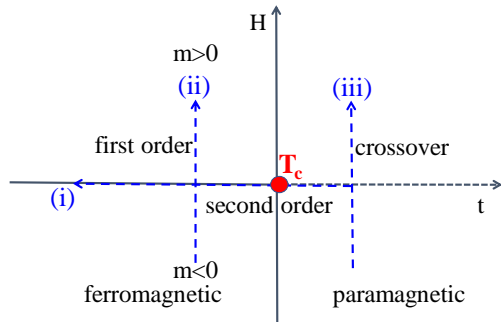


FIG. 1: Phase diagram of the 3D Ising model.

Ising model. We first demonstrate that deep neural network can learn thermodynamical observables such as average magnetization or energy. With a unique network architecture, it can identify both the second- and the first-order phase transitions in the phase diagram of the Ising model. The important features for classification of different types of phase transitions in the network are extracted. The rest of the paper is organized as follows. In Sec. II we give a brief description of the 3D Ising model and its phase structure, explaining the ML method to learn the spin configurations in the model. The results of identifying different types of phase transitions in the Ising model are reported and discussed in Sec. III. Our findings are summarized in Sec. IV.

II. THE ISING MODEL AND MACHINE LEARNING METHOD

The Ising model [54] is regarded as one of the most fundamental magnetic models to study the nature of phase transitions from a microscopic viewpoint in statistical physics. The energy of the 3D Ising model is given by

$$E = -H \sum_i \sigma_i - J \sum_{\langle ij \rangle} \sigma_i \sigma_j. \quad (1)$$

Here σ_i is the spin of the i th site. It equals either 1 (spin up) or -1 (spin down). We consider the model on a cubic lattice with periodic boundary conditions and set $J = 1$ as the energy unit. The first sum describes the interaction of the spins with an external magnetic field H . The energy is minimum when a spin points parallel to the external magnetic field. The second sum is taken only over pairs (i, j) that are nearest neighbors in the grid, and it describes the interaction of the spins with each other. The interaction energy of a pair of adjacent spins is minimum when they point in the same direction. We usually normalize quantities of interest by the number of degrees of freedom and then work with the average energy per spin, $\epsilon = \langle E \rangle / N$, and the average magnetization per spin, $m = \frac{1}{N} \langle \sum_i \sigma_i \rangle$. The average magnetization can be regarded as the order parameter of this model.

The phase diagram of the 3D Ising model [34, 37] is shown in Fig. 1. The horizontal and vertical axes in the figure are reduced temperature $t = (T - T_c) / T_c$ and external magnetic field H , respectively. When decreasing temperature under zero magnetic field, i.e. along the direction of line (i) as shown in the plot, a second-order phase transition with spontaneous twofold symmetry breaking occurs at the critical point T_c . A discrete $Z(2)$ spin inversion symmetry is broken in the ferromagnetic (order) phase below T_c and is restored in the paramagnetic (disordered) phase at temperatures above T_c . On the other hand, when we change the external magnetic field with fixed temperature below T_c , i.e. along the direction of line (ii), a first-order phase transition occurs between two phases corresponding to $m < 0$ and $m > 0$. The stable phase is the one for which m has the same sign as H , but the magnetization remains nonzero even in the limit $H \rightarrow 0$. The system therefore undergoes a first-order phase transition in which m changes discontinuously as it crosses the coexistence curve at $H = 0$. The size of the discontinuity decreases with increasing temperature, and it reaches zero at the critical temperature T_c , i.e., the coexistence curve ends at a critical point. When we change the external magnetic field with fixed temperature beyond T_c , i.e. along the direction of line (iii), the transition will be a smooth crossover. According to a non-universal mapping between Ising variables (t, H) and QCD coordinates (T, μ_B) in the phase diagrams, we can construct an equation of state matching the first principle Lattice QCD calculations, which can be employed in hydrodynamic simulations in relativistic heavy-ion collision [32–35].

The Monte Carlo (MC) simulation of the 3D Ising model on size $L \times L \times L$ is implemented by the Metropolis algorithm. This algorithm is a simple and widely used approach to generate the canonical ensemble. It allows to efficiently obtain a large number of uncorrelated sample configurations over a wide temperature range. We generate 20000 independent spin configurations at each selected temperature and external magnetic field. About 90% event samples are randomly chosen as inputs for training the ML model and the rest for testing its performance. In order to reduce correlations of samples, we take 50 sweeps between every two independent configurations [55].

ML as a tool for analysing data is becoming more and more prevalent in an increasing number of fields. Supervised learning, as one of the common used method, is performed with prior knowledge of the correct output values for a subset of given inputs. In this case, the objective is to find a function that best approximates the relationship between input and output for the dataset. Then the trained machine can recognize unseen samples and predict their associated label, demonstrating that it has learned by generalizing the samples that it has not encountered before.

In deep learning, a convolutional neural network (CNN) [53] is a class of deep neural network, mostly

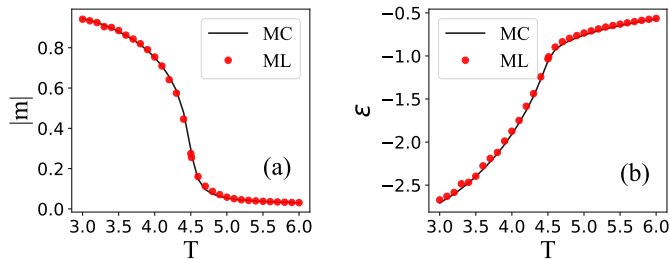


FIG. 2: (a) The average absolute value of magnetization and (b) average energy obtained by predictions of the 3D CNNs (red dots) and Monte Carlo simulations (black lines).

applied to analyze visual imagery. It is inspired by biological processes in which the connectivity pattern between neurons resembles the organization of the animal visual cortex. The CNN is known as shift or space invariant of multilayer perceptrons. It has the distinguishing features of local connectivity, shared weights, pooling, etc. Motivated by previous studies [56–59], we apply ML techniques to the 3D Ising model. The supervised learning with deep CNN architecture is used to explore phase transitions and phase structure of the system.

III. RESULTS AND DISCUSSIONS

A. ML the average magnetization and energy

In thermodynamics, a phase transition occurs when there is a singularity in the free energy. In the Ising model, calculations of the average energy of various spin configurations will help to obtain free energy. Then a standard recipe can be followed to find all other quantities of interest. The other important macroscopic quantity that describes the system is the average magnetization (order parameter). Phase transitions often involve the development of some type of order with an associated symmetry breaking. The broken symmetry is described by an order parameter usually increases on moving deeper into the ordered phase, and which measures the degree of order as the phase transition proceeds.

We perform a supervised learning for spin configurations in the 3D Ising model. The input data for ML networks are obtained from Monte Carlo sampling at different temperatures at vanishing magnetic field in a cubic lattice $L = 16$. The spin configurations are labeled by their corresponding average absolute value of magnetization or average energy, respectively. The data sets are randomly divided into the train and test sets. The supervised machine learning networks are trained in the train sets and predicted in the test sets. In this work, we adopt a 3D CNN architecture which is based on Tensorflow 2.0 and implemented with Keras library.

We train 3D CNNs to predict average absolute value of magnetization and energy and the results are shown in

Fig. 2 (a) and (b), respectively. The red dots represent the predictions from the 3D CNNs and the black solid lines are the calculations from Monte Carlo simulations. The predicted average magnetization and energy of different spin configurations from 3D CNNs agree very well with the Monte Carlo simulations. It means that the machine can learn physical quantities of order parameter and energy from pure spin configurations in the Ising model.

B. ML the second-order phase transition

We now consider the ability of ML to identify phase transitions in the 3D Ising model. As described in Sec. II, the second-order phase transition of the 3D Ising model occurs at a critical temperature T_c . It separates a ferromagnetic phase, characterized by a nonzero average magnetization per spin, from a featureless paramagnetic phase at high temperatures. For a given cubic size lattice, each sample in the Monte Carlo simulations is binary labeled with its corresponding phase, i.e., high-temperature disorder phase when $T > T_c$ and low-temperature order phase when $T < T_c$. This allows us the opportunity to attempt to classify the two different types of configurations without use of any thermodynamical estimators. The problem of identifying the phase for a certain value of the temperature is then reformulated as a classification problem in ML.

We construct a 3D CNN to perform supervised learning directly on the uncorrelated raw configurations sampled by Monte Carlo. The numerical results obtained at various system sizes are illustrated in Fig. 3 (a). It is found that the average outputs of different sizes cross at a temperature around 4.51, which is very close to Monte Carlo simulations [60, 61]. The CNN model successfully classifies the high- and low-temperature phases. The result does solely base on the raw spin configurations without providing any other thermodynamical quantities. The overall accuracies obtained from the test sets with different system sizes L are shown in Fig. 3 (c). The prediction accuracy increases from 86.3% (for $L = 8$) to 96.7% (for $L = 28$).

Critical exponents of the 3D Ising model are important physical quantities to describe the critical behavior of phase transitions. They are universal, i.e. they do not depend on the details of the physical system. If the critical point of QCD exists, it may well be that its actual critical exponents are those of the 3D Ising model. We take a finite-size scaling analysis [62] to obtain the critical exponent ν by using the outputs of different sizes in $L \in [8, 28]$. The results are shown in Fig. 3 (b). The data points of various sizes collapse with each other with the critical exponent $\nu = 0.63$, which agrees very well with the results obtained from the renormalization group theory [63] and Monte Carlo method [64]. Therefore, ML can not only detect phases and locate the transition temperature T_c , but also obtain the critical exponent of the

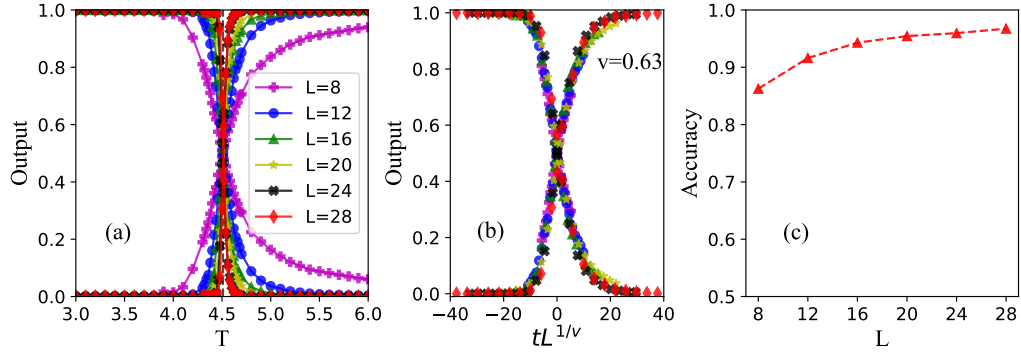


FIG. 3: (a) The output layer averaged over test sets as a function of temperature at six different system sizes. (b) Plot showing data collapse of the average output layer as a function of $tL^{1/\nu}$, where $t = (T - T_c)/T_c$ is the reduced temperature. (c) The overall accuracies as a function of L .

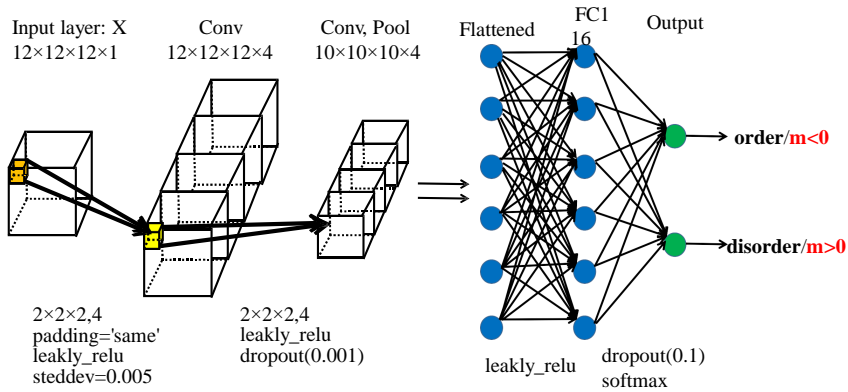


FIG. 4: The 3D convolutional neural network architecture used in present analysis.

3D Ising model.

The detail CNN architecture used in this analysis is shown in Fig. 4. The network is composed of a 3D input layer, two 3D convolutional layers, a pooling layer, a fully connected hidden layer, and an output layer. In addition, the pooling layer and fully connected hidden layer follow by a dropout layer with rate 0.001 and 0.1 respectively. In the first convolutional layer, there are 4 filters with size $2 \times 2 \times 2$ and stride $s = 1$ to apply the input configurations and create activations. These activations are further convoluted in the second convolutional layer that has the same number, size, and stride of filters as in the first convolutional layer. The second convolutional layer is then forwarded by a pooling layer of size $2 \times 2 \times 2$ and stride $s = 1$. The fully connected layer has 16 neurons and the output layer is another fully connected layer with softmax activation and two neurons to indicate the result of classification. In this work, all the layers are activated by LeaklyReLU functions except for the output layer. The mean-square error function is used as loss function, and the Adam optimizer is exploited to update the weights and biases.

C. ML the first-order phase transition

The power of neural networks lies in their ability to generalize to tasks beyond their original design. In previous subsection, we have constructed a 3D convolutional neural network to successfully identify the second-order phase transition in the 3D Ising model. We want to know if the same network architecture can also be used to discriminate the first-order transition in the model.

From the phase diagram of the Ising model as demonstrated in Fig. 1, the first-order phase transition takes place when one changes the external magnetic field H across the transition boundary $H = 0$ with $T < T_c$. In order to study the effect of temperature on this transition, we generate event samples by taking two different temperatures of $T = 3.60$ (far away from the critical temperature T_c) and $T = 4.50$ (near T_c). The same 3D CNN architecture as illustrated in Fig. 4 is used to train and make predictions on the test sets for both cases. The results are shown in Fig. 5 (a) and (b), respectively. The CNN architecture, which is originally constructed to identify the second-order phase transition, can successfully classify the $m > 0$ and $m < 0$ phases, too. The

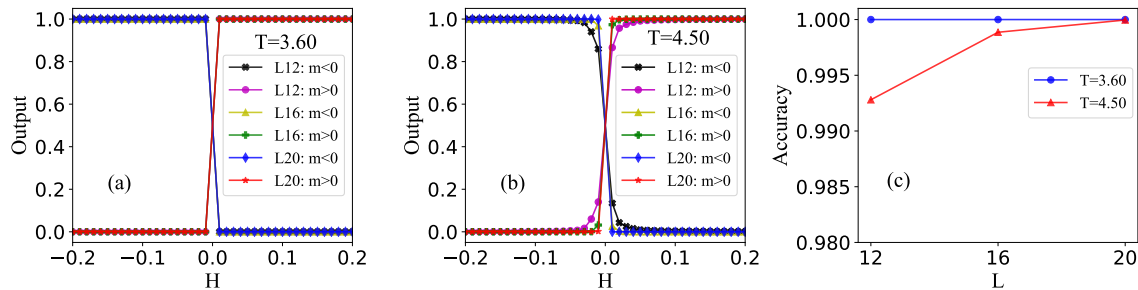


FIG. 5: The output layer averaged over test sets as a function of external magnetic field at three different system sizes at (a) $T = 3.6$ and (b) $T = 4.5$. (c) The overall accuracies as a function of L at two different temperatures.

average outputs of three different sizes cross exactly at $H = 0$ in both cases. The test accuracies with different system sizes are shown in Fig. 5 (c). When the temperature of the system is far away from T_c , the network can classify phases perfectly (blue dots). And the accuracy decreases with the decreasing system size when the temperature is near T_c (red triangles). This is due to the effect of large critical fluctuations when the system is near the temperature where the second-order phase transition occurs.

D. Exploration of the important features in the CNN

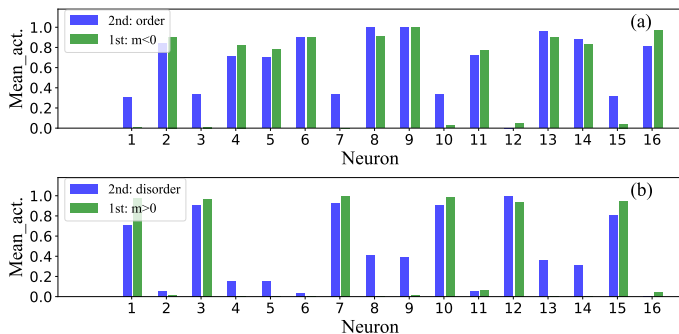


FIG. 6: Mean activations at the 16 hidden neurons in the fully connected layer of the 3D Ising-trained convolutional neural network for configurations from the second-order (blue bars) and the first-order (green bars) phase transitions.

In statistical physics, the second-order phase transition is a continuous transition but the first-order phase transition is a discontinuous one. They belong to different types of phase transitions and have different equations of state. Here it has been shown that the CNN architecture constructed in this paper can identify both the second- and the first-order ones in the 3D Ising model. The great advantage of the DL method is the ability to extract hidden features from highly dynamical, rapidly evolving and complex non-linear systems, like in the Ising model or in the relativistic heavy-ion collisions [46]. The neural net-

work should itself select the appropriate features within the data which are most sensitive to the properties of different types of equations of state.

In order to get physical insights of how the neural network discriminate the two types of phase transitions, it is instructive to visualize the complex dependence learned by the network. DL uses multiple layers of representation to learn descriptive features directly from training data. The important features, which used in the classification process for phase transitions and for identifying any underlying physical quantities, may be encoded in the convolutional filter kernels [65], the weight matrices [57, 65, 66], or the activations of the hidden units in the network [67]. The sets of variational parameters, specifically the weights and the biases at each layer of the neural network, are optimized during the training process. They will converge to certain values which encode the solution to the particular problem under consideration. Within the shallow layers of a network architecture, the variational parameters correspond to learned universal features. This form of universality is diminished towards deeper layers where the features are expected to transit from universal to specific in relation to different systems. The activation function of a variable in an intermediate layer of the neural network acts as a transformation that maps a certain input to an output representation [67].

We calculate the mean activation functions of neural network configurations from different types of phase transitions. The results are shown in Fig. 6, where the activations have been drawn for 16 neurons of the fully connected layer as depicted in Fig. 4. The blue and green bars are the calculations from the second- and the first-order phase transitions, respectively. The maximum value has been normalized to one, and the results have been rescaled accordingly for better representation. We observe that the number of non-zero blue bars is more than that of green ones. The activations show a rather broader spread of values in the second-order phase transition than in the first-order one. It infers that more neurons are activated in the classifying tasks of the second-order phase transition due to large fluctuations near the critical point in this transition. The growth of the acti-

vated hidden neurons at criticality may also be reminiscent of the connection between DL and the renormalization group [68, 69].

IV. CONCLUSIONS AND OUTLOOK

In this paper, we have employed a supervised learning method to study phase transitions in the 3D Ising model. It is found that a 3D convolutional neural network can be trained to predict average magnetization and average energy with high accuracies. The network successfully classifies high- and low-temperature phases of the 3D Ising model. It is able to not only locate the transition temperature but also obtain the critical exponent of the second-order phase transition based on the raw spin configurations without providing any other thermodynamical quantities. With the same CNN architecture, the neural network can identify different phases in the first-order transition with high accuracies. This implies that the network spontaneously captures both the second- and the first-order phase transitions and encodes it in the machine parameters during the process of supervised learning. Furthermore, we have tried to extract and decode important features of the classification processes directly from the data. It is found that the activations in the high-level representations show a broader spread of values in the second-order phase transition than in the first-order one due to large fluctuations at the critical point.

In relativistic heavy-ion collisions, we expect the QCD

critical point to have similar critical behaviors as those in the 3D Ising model due to the same universality that is dictated by the symmetry of the systems. In heavy-ion experiments, the measured high-order cumulants [15, 70, 71] and intermittency [72–74] both at SPS and RHIC energies suggest that there exists large density fluctuations near the QCD critical point. Here we have proved that the state-of-the-art ML method can learn the important features which discriminate different types of phase transitions. Understanding what this approach captures will be useful when we explore the QCD critical point and phase boundary experimentally. The method developed in this study can also be applied to investigate the criticality in Monte-Carlo models, which could help to explore physical mechanisms of the QCD phase transition.

Acknowledgments

We are grateful to Prof. Yuanfang Wu, Mingmei Xu and Longgang Pang for their fruitful discussions and comments. We further thank Prof. Hengtong Ding for providing us with computing resources. The numerical simulations have been performed on the GPU cluster in the Nuclear Science Computing Center at Central China Normal University (NSC³). This work is supported by the Ministry of Science and Technology (MOST) under Grant No. 2016YFE0104800.

X.L. and R.G. contributed equally to this work.

-
- [1] M. A. Stephanov, K. Rajagopal, and E. V. Shuryak, *Phys. Rev. Lett.* 81, 4816 (1998).
 - [2] J. Adams *et al.* (STAR Collaboration), *Nucl. Phys. A* 757, 102 (2005).
 - [3] M. Asakawa, U. W. Heinz, and B. Muller, *Phys. Rev. Lett.* 85, 2072 (2000).
 - [4] V. Koch, A. Majumder, and J. Randrup, *Phys. Rev. Lett.* 95, 182301 (2005).
 - [5] Y. Aoki *et al.*, *Nature* 443, 675 (2006).
 - [6] Y. Aoki *et al.*, *Phys. Lett. B* 643, 46 (2006); M. Cheng *et al.*, *Phys. Rev D* 74, 054507 (2006).
 - [7] E.S. Bowman and J.I. Kapusta, *Phys. Rev. C* 79, 015202 (2009); S. Ejiri, *Phys. Rev. D* 78, 074507 (2008).
 - [8] M.A. Stephanov, *Prog. Theor. Phys. Suppl.* 153, 139 (2004); Z. Fodor and S.D. Katz, *JHEP* 04, 50 (2004).
 - [9] R.V. Gavai and S. Gupta, *Phys. Rev. D* 78, 114503 (2008); *Phys. Rev. D* 71, 114014 (2005).
 - [10] M. A. Stephanov, *Phys. Rev. Lett.* 102, 032301 (2009).
 - [11] M. A. Stephanov, *Phys. Rev. Lett.* 107, 052301 (2011).
 - [12] B. J. Schaefer and M. Wagner, *Phys. Rev. D* 85, 034027 (2012).
 - [13] S. Gupta, X. Luo, B. Mohanty, H. G. Ritter and N. Xu, *Science* 332, 1525 (2011).
 - [14] M. M. Aggarwal *et al.* (STAR Collaboration), *Phys. Rev. Lett.* 105, 022302 (2010).
 - [15] L. Adamczyk *et al.* (STAR Collaboration), *Phys. Rev. Lett.* 112, 032302 (2014).
 - [16] L. Adamczyk *et al.* (STAR Collaboration), *Phys. Rev. Lett.* 113, 092301 (2014).
 - [17] L. Adamczyk *et al.* (STAR Collaboration), *Phys. Lett. B* 785, 551 (2018).
 - [18] A. Adare *et al.* (PHENIX Collaboration), *Phys. Rev. C* 93, 011901 (2016).
 - [19] X. Luo (for the STAR Collaboration), *PoS CPOD2014*, 019 (2015).
 - [20] X. Luo and N. Xu, *Nucl. Sci. Technol.* 28, 112 (2017).
 - [21] A. Bzdak, *et al.*, *Phys. Rep.* 853, 1 (2020).
 - [22] R. Pisarski, *et al.*, *Phys. Rev. D* 29, 338 (1984).
 - [23] F. Karsch, E. Laermann, and Ch. Schmidt, *Phys. Lett. B* 520, 41 (2001).
 - [24] S. Gavin, A. Gocksch, and R. D. Pisarski, *Phys. Rev. D* 49, R3079 (1994).
 - [25] M. A. Halasz, A. D. Jackson, R. E. Shrock, M. A. Stephanov, and J. J. M. Verbaarschot, *Phys. Rev. D* 58, 096007 (1998).
 - [26] J. Berges and K. Rajagopal, *Nucl. Phys. B* 538, 215 (1999).
 - [27] Ch. Schmidt, F. Karsch, E. Laermann, and, *Nucl. Phys. B* 106, 423 (2002).
 - [28] C. Alexandrou *et al.*, *EPJB* 93, 226 (2020).

- [29] C. Giannetti, B. Lucini and D. Vadacchino, Nucl. Phys. B 944, 114639 (2019).
- [30] A. Kiyohara, et al., arXiv:2108.00118.
- [31] F. Gliozzi and A. Rago, JHEP 10, 042 (2014).
- [32] M. Pradeep and M. Stephanov, Phys. Rev. D 100, 056003 (2019).
- [33] P. Parotto, Nucl. Phys. A 982, 183 (2019).
- [34] P. Parotto, et al., Phys. Rev. C 101, 034901 (2020).
- [35] D. Mroczek, et al., Phys. Rev. C 103, 034901 (2021).
- [36] P. Parotto, PoS CPOD2017, 036 (2017).
- [37] R. Tamura, et al., arXiv:1111.6509.
- [38] A. Kitaev, Ann. Phys. 303, 2 (2003).
- [39] X. Wen, Int. J. Mod. Phys. B 04, 239 (1990).
- [40] G. E. Hinton and R. R. Salakhutdinov, Science 313, 504 (2006).
- [41] Y. LeCun, Y. Bengio, and G. Hinton, Nature (London) 521, 436 (2015).
- [42] P. Mehta, M. Bukov, C.-H. Wang, A. G. R. Day, C. Richardson, C. K. Fisher, and D. J. Schwab, Phys. Rep. 810, 1 (2019).
- [43] G. Carleo, et al., Rev. Mod. Phys. 91, 045002 (2019).
- [44] L.-G. Pang, K. Zhou, N. Su, H. Petersen, H. Stocker, and X.-N. Wang, Nature Commun. 9, 210 (2018).
- [45] L.-G. Pang, Nucl. Phys. A 1005, 121972 (2021).
- [46] Y.-L. Du, K. Zhou, J. Steinheimer, L.-G. Pang, A. Motornenko, H.-S. Zong, X.-N. Wang, and H. Stocker, Eur. Phys. J. C 80, 516 (2020).
- [47] Y. Kvasiuk, E. Zabrodin, L. Bravina, I. Didur, and M. Frolov, JHEP 07, 133 (2020).
- [48] J. Steinheimer, L. Pang, K. Zhou, V. Koch, J. Randrup, and H. Stoecker, JHEP 12, 122 (2019).
- [49] M. O. Kuttan, K. Zhou, J. Steinheimer, A. Redelbach, and H. Stoecker, JHEP 10, 184 (2021).
- [50] R. Wang, Y.-G. Ma, R. Wada, L.-W. Chen, W.-B. He, H.-L. Liu, and K.-J. Sun, Phys. Rev. Res. 2, 043202 (2020).
- [51] S. S. Schoenholz, E. D. Cubuk, D. M. Sussman, E. Kaxiras, and A. J. Liu, Nat. Phys. 12, 469 (2016).
- [52] P. Broecker, J. Carrasquilla, R. G. Melko, and S. Trebst, Sci. Rep. 7, 8823 (2017).
- [53] I. Goodfellow, Y. Bengio, and A. Courville, Deep Learning (MIT Press, Cambridge, MA, 2016).
- [54] E. Ising, Z. Physik 31, 253 (1925).
- [55] M. and G. Barkema, Monte carlo methods in statistical physics (Oxford University Press, 1999).
- [56] J. Carrasquilla and R. G. Melko, Nat. Phys. 13, 431 (2017).
- [57] A. Tanaka and A. Tomiya, J. Phys. Soc. Jpn. 86, 063001 (2017).
- [58] Z. Li, M. Luo, and X. Wan, Phys. Rev. B 99, 075418 (2019).
- [59] R. Zhang, et al., Phys. Rev. B 99, 094427 (2019).
- [60] A. Talapov and H. Blote, J Phys. A 29, 5727 (1996).
- [61] G. S. Pawley, R. H. Swendsen, D. J. Wallace, and K. G. Wilson, Phys. Rev. B 29, 4030 (1984).
- [62] V. Privman, Finite Size Scaling and Numerical Simulation of Statistical Systems (Wolrd Scientific, 1990)
- [63] A. Pelissetto and E. Vicari, Phys. Rep. 368, 549 (2002).
- [64] K. Binder, E. Luijten, Phys. Rep. 344, 179 (2001).
- [65] P. Suchsland and S. Wessel, Phys. Rev. B 97, 174435 (2018).
- [66] K. Kashiwa, Y. Kikuchi and A. Tanaka, Prog. Theor. Exp. Phys., 083A04 (2019).
- [67] D. Bachtis, G. Aarts and B. Lucini, Phys. Rev. E 102, 053306 (2020).
- [68] G. Torlai and R. G. Melko, Phys. Rev. B 94, 165134 (2016).
- [69] P. Mehta and D. J. Schwab, arXiv:1410.3831.
- [70] J. Adam *et al.* (STAR Collaboration), Phys. Rev. Lett. 126, 092301 (2021).
- [71] M. Abdallah *et al.* (STAR Collaboration), Phys. Rev. C 104, 024902 (2021).
- [72] T. Anticic *et al.* (NA49 Collaboration), Eur. Phys. J. C 75, 587 (2015).
- [73] D. Prokhorova *et al.* (NA61 Collaboration), universe 5050103 (2019).
- [74] J. Wu *et al.* (for the STAR Collaboration), presentation at ISMD2021, virtual conference, 12-16 July 2021.